Preprints of the 19th World Congress
The International Federation of Automatic Control
Cape Town, South Africa. August 24-29, 2014

Optimal Selection of Driving Modes along a Commuter Route for a Plug-in Hybrid Electric Vehicle

Andreas Furberg * **Viktor Larsson** ** **Bo Egardt** **

* *andfur@student.chalmers.se*
** *{lviktor,egardt}@chalmers.se*
Chalmers University of Technology, Göteborg, Sweden

Abstract: Many plug-in hybrid electric vehicles have predefined driving modes, e.g. electric drive and charge sustaining mode. For a driver it is not a trivial task to select a fuel optimal sequence of driving modes; a poor selection might even result in a severely degraded fuel economy. The purpose of this paper is therefore to investigate optimal mode selection along a well known commuter route. To obtain a predictable driving behaviour it is assumed that the driving mode is only allowed to change at a limited number of decision points, located where the driving conditions along the route changes. The optimal mode selection is computed using the well known Dynamic Programming algorithm. However, the results show that the optimal mode selection might be perceived as counterintuitive, as a mode is not necessarily optimal over a connected set with respect to battery state of charge, at a given decision point. To mitigate this type of behaviour a suboptimal algorithm is proposed, in which a mode is associated with one unique interval of state of charge at any decision point along the route. The results indicate that the proposed algorithm is only marginally suboptimal with respect to the optimal solution.

Keywords: Plug-in Hybrid Electric Vehicle, Optimal Control, Dynamic Programming

1. INTRODUCTION

Driveability is an important concept for automotive manufacturers, as it is very noticeable for the customer and the overall driving experience. However, within the academic community driveability has often been neglected since it is a somewhat vague concept. Instead the focus has been on optimal fuel economy and sophisticated energy management strategies have been developed. Often based on optimal control methods such as the Pontryagin Minimum Principle and Dynamic Programming (DP), see Sciarretta and Guzzella (2007); Wirasingha and Emadi (2011) for a review of different methods. Some authors have nevertheless taken drivability into account when formulating the optimal control problem. Pisu et al. (2005) suggests a Linear Quadratic Regulator as a method to minimize driveline vibrations and obtain smooth gear shifts. In Opila et al. (2008, 2012) gear shifts and engine on/off events are penalized by artificial costs in a Stochastic DP formulation. Furthermore, in Johannesson et al. (2009) the engine on/off decision is optimized using DP with respect to a set of predicted scenarios that might occur during the next few seconds of driving.

The aim of this paper is also related to drivability, but the focus is slightly different compared to the previously mentioned papers. The authors recognize that it is common practice within the automotive industry to predefine different driving modes, e.g. *Sport, Eco, Electric Drive, Charge Sustaining* etc. These driving modes are typically defined by heuristic rules to satisfy perceived driveability constraints defined by the manufacturer. The idea is that the vehicle should behave consistently within each mode, so that the driver can anticipate the behaviour reasonably well. Typically, it is up to the driver to decide the driving mode; however, for a Plug-in Hybrid Electric Vehicle (PHEV) it is not a trivial task to select a fuel optimal sequence of driving modes, e.g. when to drive in *Electric Drive* or in *Charge Sustaining* mode. Consequently, a poor selection of driving modes can easily result in an increased fuel consumption.

The main idea in the paper is therefore to consider a PHEV with rule-based driving modes, deciding torque split, gear selection and engine state, and instead optimize the selection of driving modes along a frequently driven commuter route. Moreover, to ensure some form of predictability for the driver, the driving mode is only allowed to change at a limited number of decision points along the route. The decision points are placed at positions along the route where the driving conditions change, e.g. from urban to highway driving or from uphill to downhill. With this approach it is possible to obtain the best possible fuel economy while using the rule-based modes, defined by the vehicle manufacturer to ensure driveability and predictability.

The methodology in the paper is to consider a simple quasi-static model of a PHEV, having three different rule based driving modes. A real world commuter route is investigated using several weeks of logged driving data; approximately thirty decision points are identified for the 60 km long route. DP is then used to precompute a look-up-table for the optimal mode selection at the different decision

points along the route. The mode selection obtained with DP might, however, be experienced as counterintuitive for a commuter driving along the route on a daily basis, as the optimal mode at a specific decision point is not always consistent with respect to the battery State of Charge (SoC) level. Therefore a slightly sub-optimal mode selection algorithm is proposed; the algorithm ensures that the mode selection is consistent with respect to battery SoC level; something which is not guaranteed with conventional DP.

Paper Outline: The paper is divided into seven sections. After the introduction the vehicle model and the driving modes are explained. The next section presents the investigated commuter route along with the identified decision points. In the following section the optimal mode selection problem is solved with Dynamic Programming and the suboptimal mode selection algorithm is presented. The paper is then ended with a simulation study and some conclusions.

2. VEHICLE CONFIGURATION AND MODELLING

The vehicle configuration considered in this paper is a simplified model of the Volvo V60 PHEV, which is a parallel hybrid. The electric motor powers the rear axis while the diesel engine powers the front axis. At high speeds the motor can be declutched from the powertrain to decrease the drag losses. Furthermore, the engine can also be used to power the generator and thereby recharge the battery. A schematic illustration of the configuration is depicted in Figure 1, and the key powertrain components are summarised in Table 1.

2.1 Powertrain Model

This section presents the mathematical model of the powertrain and the key powertrain components.

Engine: At a given speed, ω_{ice}, the mass fuel rate, $\dot{m}_f$, of the Internal Combustion Engine (ICE) is assumed affine in torque

$$\dot{m}_f = (c_0(\omega_{ice})T_{ice} + c_1(\omega_{ice}))e_{on}, \tag{1}$$

where e_{on} is the binary engine state. The coefficients $c_{0:1}$ are speed dependent and determined by linear least squares from the brake specific fuel consumption map.
Electric Motor: The Electric Motor (EM) is placed at the rear axis and is modelled jointly with the inverter; the combined electrical power is assumed quadratic in motor torque

$$P_{em} = d_0(\omega_{em})T_{em}^2 + d_1(\omega_{em})T_{em} + d_2(\omega_{em}). \tag{2}$$

The coefficients $d_{0:2}$ are speed dependent and are determined by linear least squares from the power loss maps of the EM and the inverter. The torque is defined positive in motoring mode and negative in generator mode.
Integrated Starter Generator: The generator (or Integrated Starter Generator - ISG) is modelled jointly with its inverter; the combined electrical power is assumed quadratic in generator torque

$$P_{isg} = e_0(\omega_{isg})T_{isg}^2 + e_1(\omega_{isg})T_{isg} + e_2(\omega_{isg}). \tag{3}$$

The coefficients $e_{0:2}$ are speed dependent and are determined by linear least squares from the power loss maps of the ISG and the inverter. Furthermore, the ISG is assumed to only operate in generator mode, i.e. $T_{isg} \leq 0$.

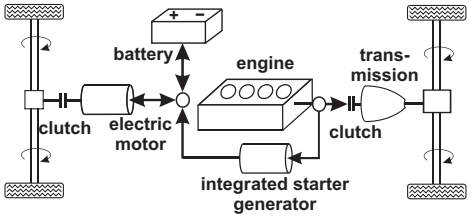

Fig. 1. A schematic illustration of the vehicle model used which is a simplified model of the Volvo V60 PHEV.

Battery: The battery is modelled as an equivalent circuit with a constant internal resistance in series with a voltage source. The open circuit voltage is assumed to be affine in the state x, i.e. SoC. The battery state dynamics are thus given by

$$\frac{dx}{dt} = -\frac{I}{Q} = -\frac{V_{oc}(x) - \sqrt{V_{oc}(x)^2 - 4R_{in}P_{bat}}}{2R_{in}Q}, \tag{4}$$

where Q denotes the cell capacity. The battery power is given by

$$P_{bat} = P_{em} + P_{isg} + P_{aux}, \tag{5}$$

and the battery power limits are imposed as speed dependent torque constraints on the EM and ISG.
Transmission Front Axis: The final drive has a gear with fixed ratio r_{fw} and a constant efficiency η_{fw}. The gearbox has fixed gear ratios $r_{gb,i}$, $i = 1, ..., 6$, with torque losses that are given by a look-up-table, $T_{gb,loss}(\omega_{wh}, r_{gb.i}, e_{on})$.
Rear Axis: The final drive has a gear with fixed ratio r_{rw} and a constant efficiency η_{rw}. The mechanical drag losses are given by a look-up table, $T_{drag,rear}(\omega_{wh}, c_{rw})$, where c_{rw} represents the clutch state at the rear axis.
ICE – ISG: A belt driven gear with a fixed ratio r_{isg} and a constant efficiency η_{isg}.
Main Powertrain Equations: The forces acting on the powertrain are calculated using an inverse simulation approach, meaning that the torque demanded at the wheels, T_d, to follow a given velocity and road slope trajectory is determined by

$$T_d = r_\omega(0.5\rho_a C_d A_f v^2 + mg(f_r \cos\theta + \sin\theta) + m_e a) \tag{6}$$

where r_w represents wheel radius, v velocity, a acceleration, θ road slope, m vehicle mass and m_e equivalent vehicle mass, i.e. including moments of inertia of the rotating parts. Hence, the main torque equation is

$$T_{\text{tot}} = T_d + T_{gb,loss,i} + T_{drag,rear} = \eta_{rw}r_{rw}T_{em} + \eta_{fw}r_{fw}r_{gb,i}(T_{ice} + \frac{r_{isg}}{\eta_{isg}}T_{isg}). \tag{7}$$

If the ICE is on, the input torque to the transmission is positive, i.e. $T_{ice} + \frac{r_{isg}}{\eta_{isg}}T_{isg} \geq 0$.

3. PHEV DRIVING MODES

In the Volvo V60 PHEV there are three principal driving modes; *Pure, Hybrid* and *Power*. In addition it is possible to activate *Save* which is not defined as a mode by the manufacturer; it can, however, in an energy management context also be considered as a mode. The *Power* mode is not treated in this paper since it emphasises performance, e.g. acceleration and vehicle dynamics, rather than fuel

Table 1. The main vehicle data.

Chassis	**Data**
Mass (m)	1930 kg
Transmission	6 Stepped Automatic
Auxiliary Load (P_{aux})	325 W
Battery	**Li-Ion**
Capacity	11.2 kWh
Engine	**5 Cyl. Diesel**
Max Power/Torque	158 kW, 440 Nm
Electric Motor	**Permanent Magnet**
Max Power/Torque	50 kW, 200 Nm
Generator (ISG)	**Permanent Magnet**
Max Power	$\approx$ 20 kW

economy. The driving modes considered in this paper are by Volvo [1] described as follows:

Pure: *"The diesel engine shuts off, letting the electric motor do all the work, (...) so that you can drive in silence with zero tailpipe emissions."*
Hybrid: *"Both the engine and the electric motor work in symbiosis for you. (...) Letting you appreciate the journey, without unnecessary stops and interruptions."*
Save: *"The diesel engine will recharge the battery to a level where you will be able to drive up to 20 km on pure electricity at a later occasion."*

3.1 Driving Mode Modelling

The modelling assumptions for the three modes are described next. Note that these assumptions are made by the authors and do not reflect the exact behaviour of the actual modes in the Volvo V60 PHEV.

Pure Both the engine and the generator are declutched and the electrical motor delivers all traction torque,

$$e_{on} = 0 \implies T_{ice} = 0,\, T_{isg} = 0$$
$$T_{em} = \begin{cases} \frac{T_{\text{tot}}}{r_{rw}} \cdot \frac{1}{\eta_{rw}} & \text{if } T_{tot} \geq 0 \\ \frac{T_{\text{tot}}}{r_{rw}} \cdot \eta_{rw} & \text{if } T_{tot} < 0. \end{cases} \tag{8}$$

If the EM cannot meet the torque request the mode is automatically changed to *Hybrid*.

Hybrid The engine is started when the power request exceeds a higher threshold value; the engine is then kept on until the power request drops below a lower threshold value. The engine state e_{on}^j, at a time sample j, is thus given by,

$$e_{on}^j = \begin{cases} 1 & \text{if } P_d \geq P_{on}(x) \\ 1 & \text{if } e_{on}^{j-1} = 1 \text{ and } P_d \geq P_{off}(x) \\ 0 & \text{if } P_d \leq P_{off}(x) \\ 0 & \text{if } e_{on}^{j-1} = 0 \text{ and } P_d \leq P_{on}(x) \end{cases} \tag{9}$$

where P_d is the current power demand. P_{on} and P_{off} are the power thresholds for turning the engine on and off, the values are SoC dependent and are illustrated in Figure 2. When the engine is on, $e_{on}^j = 1$, the operating points are:

$$\begin{aligned} T_{isg} &= \frac{0.2 - \min(\max(x, 0.1), 0.2)}{0.1} T_{isg}^{\min} \\ T_{ice} &= \frac{T_{\text{tot}} - \frac{r_{isg}}{\eta_{isg}} T_{isg}}{\eta_{fw} r_{fw} r_{gb,i}} \\ T_{em} &= 0 \end{aligned} \tag{10}$$

[1] See: www.volvocars.com.

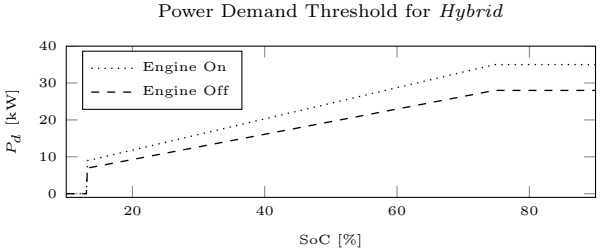

Fig. 2. Threshold values for engine on/off in *Hybrid* mode.

where $T_{isg}^{\min}$ is the lower torque constraint of the ISG. Note that the ISG will recharge the battery if the SoC drops below 20 %, thus ensuring a charge sustaining behaviour around the lower SoC limit. When the engine is off, $e_{on}^j = 0$, the operating points are:

$$\begin{aligned} &T_{isg} = 0,\, T_{ice} = 0 \\ &T_{em} = \begin{cases} \frac{T_{\text{tot}}}{r_{rw}} \cdot \frac{1}{\eta_{rw}} & \text{if } T_{tot} \geq 0 \\ \frac{T_{\text{tot}}}{r_{rw}} \cdot \eta_{rw} & \text{if } T_{tot} < 0. \end{cases} \end{aligned} \tag{11}$$

Finally the EM is declutched for speeds above 120 km/h.

Save The EM is declutched at all times which decreases drag losses at the rear axis but instead prohibits regeneration from braking and downhill driving. The operating points are:

$$\begin{aligned} e_{on} &= 1,\, T_{em} = 0 \\ T_{ice} &= \frac{T_{\text{tot}} - \frac{r_{isg}}{\eta_{isg}} T_{isg}}{\eta_{fw} r_{fw} r_{gb,i}} \\ T_{isg} &= \frac{0.4 - \min(\max(x, 0.1), 0.4)}{0.3} T_{isg}^{\min}. \end{aligned} \tag{12}$$

Note that the ISG will recharge the battery if the SoC drops below 40 %, this to ensure that up to 20 km of electrical driving is possible once *Save* is de-activated.

4. A COMMUTER ROUTE WITH DECISION POINTS

For a driver it is desirable if the mode switches along a route are both predictable and intuitive, in some sense. Consider a commuter that drives along the same route to work every day. One could argue that it would be intuitive for the driver, if the driving mode changes only at points along the route where the driving conditions tends to change. For example, it would make sense to stop electric driving and start the engine when entering a steep uphill segment or when leaving a sub-urban area to enter a highway. Hence, in this paper decision points are defined at positions along the route where either the speed profile or the road slope changes. More specifically, three velocity and three road slope classifications are defined, as indicated in Table 2.

In the paper, a specific commuter route in the western part of Sweden is considered. The route is about 60 km long and the driving conditions are very similar from day to day, as the traffic intensity in Sweden is rather low. The topographic profile and 10 logged speed profiles are depicted in Figure 3, along with the 34 identified decision points. The logged driving data is taken from the Swedish Car Movement Database, see Karlsson (2013).

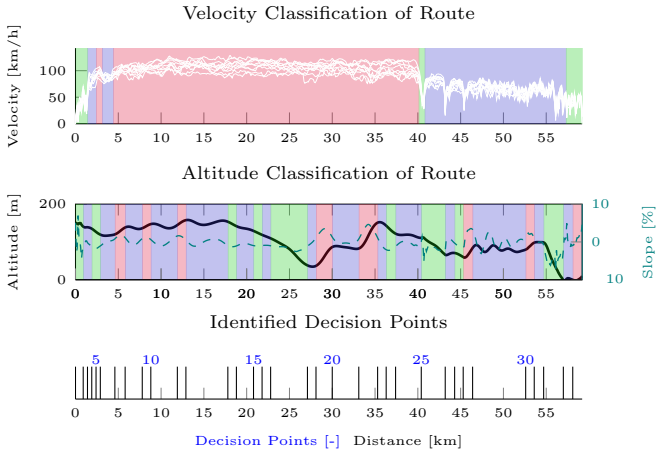

Fig. 3. The commuter route; 10 logged speed profiles are shown and the corresponding altitude profile. The lower plot depicts the identified decision points.

Table 2. The route decision points are defined by speed and road slope classifications.

Property	Decision Point Classification			Unit
	Urban	Highway	Motorway	
Velocity	< 50	$50 - 90$	> 90	km/h
	Downhill	Flat	Uphill	
Road Slope	< -1	$-1 - 1$	> 1	%

5. OPTIMAL DRIVING MODE SELECTION

Given a route with N decision points, the optimal mode selection problem can be formulated as the following optimization problem

$$J^* = \min_{u_{1:N}} \quad S(x(t_{N+1})) + \sum_{k=1}^{N} L(t, u_k) \tag{13}$$

$$s.t. \quad x(t_{k+1}) = x(t_k) + \int_{t_k}^{t_{k+1}} f\big(x(t), P_{bat}(t, u_k)\big)\ \mathrm{d}t$$

$$x(t_1) = x_{\text{init}}$$

$$x \in [x_{\min}, x_{\max}]$$

$$u_k \in \{Save, Hybrid, Pure\}.$$

The fuel cost incurred over the route segment between two consecutive decision points is given by

$$L(t, u_k) = c_f \int_{t_k}^{t_{k+1}} \dot{m}_f(t, u_k)\ \mathrm{d}t, \tag{14}$$

where c_f denotes fuel price. Note that L is completely defined by the driving mode as the operating points of the ICE, EM and ISG are decided by heuristic rules within each mode. The final cost is given by S and penalizes low final states and represents the cost to recharge the battery at the end of the route. It is defined as

$$S(x) = \max\{a_1 x + b_1,\ a_2 x + b_2\}. \tag{15}$$

5.1 Solution with Dynamic Programming

The optimal control problem defined above is a sequential problem with N steps, representing the decision points along the route where it is allowed to change driving mode. Furthermore, it is an integer decision problem, as the control signal u is the choice of driving mode. The well known Dynamic Programming algorithm is well suited to solve this type of sequential problem formulation, see Bertsekas (2000). To solve the problem with DP the SoC state, x, is gridded into m points, $x_1, ..., x_m$, and the time intervals between the decision points are time discretized with a sampling time of one second.

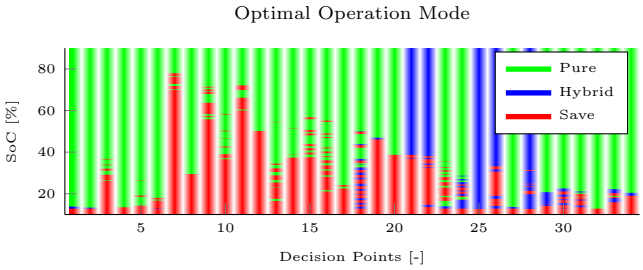

Fig. 4. The optimal driving modes at the different decision points along the route. The result is obtained with DP for one of the logged speed profiles along the route.

Then starting at the end position of the route, $k = N + 1$, the cost-to-go matrix J is initialized with the final cost S. The DP equation is thereafter solved recursively backwards over the decision points and the gridded values of the state,

$$J_k(x_i) = \tag{16}$$

$$\begin{cases} S(x_i), & k = N + 1 \\ \min\limits_{u_{k,i}} \Big\{ L(u_{k,i}) + J_{k+1}\big(x_i + \tilde{f}_k(x_i, u_{k,i})\big) \Big\}, & k \in [1, N] \end{cases}$$

where $i = 1, ..., m$ and $\tilde{f}_k(x_i, u_{k,i})$ represents the change in the state between two consecutive decision points. Thus, at each decision point k the cost-to-go is represented by a vector J_k, which is defined over the gridded values of the SoC state, $x_{1:m}$.

Figure 4 depicts the optimal driving mode at the different decision points along the route, as obtained by

$$u^*_{k,i} = \arg\min_{u_{k,i}} \big\{ L(u_{k,i}) + J_{k+1}\big(x_i + \tilde{f}_k(x_i, u_{k,i})\big) \big\}. \tag{17}$$

The results show that a specific mode is not necessarily optimal over a connected set with respect to the SoC state. This behaviour is explained mainly by the final penalty function S and the limited freedom in terms of control decisions; i.e. the torque split decision is given by heuristic rules and the number of decision points along the route is limited. Thus, to avoid a too low final state and a high final cost, the optimal mode selection might be quite intricate.

For a driver the optimal driving mode, as given by Eq. (17), might be experienced as counterintuitive. For example, consider a vehicle that is driven regularly along a commuter route. Assume that, at some day, the vehicle reaches a decision point at 50% SoC and *Pure* is selected as the optimal mode, i.e. electric driving. The following day the vehicle could reach the same decision point at a higher SoC value and *Save* might be selected as the optimal mode; thus meaning that the engine will be turned on at a higher SoC than the previous day when electric driving was selected. This would not be a predictable driving behaviour, as most drivers would expect the engine to be turned on, only if the SoC is lower than at the previous day.

5.2 A Suboptimal DP Algorithm

The solution obtained with conventional DP is not really acceptable as it might be experienced as unpredictable by a driver. Hence, to ensure some form of predictability a slightly suboptimal mode selection algorithm is proposed. The algorithm ensures that a driving mode is "optimal" over a connected set with respect to the SoC state, at each decision point. Furthermore, the mode sequence with respect to the state is fixed. *Save* at low SoC values, *Hybrid* at intermediate values and *Pure* at high values; i.e. use of the engine should be favoured as SoC decreases. The opimization variables in the proposed algorithm are the SoC threshold values where the optimal mode should change, at a given decision point.

The algorithm is described by the following steps:

(1) At the end of the route initialize the cost-to-go with the final cost S

$$\hat{J}_{N+1}(x_i) = S(x_i).\ i = 1, ..., m \tag{18}$$

(2) For all decision points $k = N, N-1, , ..., 1$ compute

$$\bar{J}_k^j(x_i) = L(u^j) + \hat{J}_{k+1}(x_i + \tilde{f}_k(x_i, u^j)), \tag{19}$$

i.e. Eq. (16) but without minimization with respect to u; thus forming three intermediate cost-to-go vectors, one for each mode $j \in \{Save, Hybrid, Pure\}$.

(3) The new cost-to-go vector, at a decision point k, is obtained by concatenating three segments of the $\bar{J}_k^j$'s. The concatenation points are given by

$$(\hat{a}, \hat{b}) = \arg\min_{(a,b)} \Big\{ \sum_{i=1}^{a} \bar{J}_k^{Save}(x_i) + \sum_{i=a+1}^{b} \bar{J}_k^{Hybrid}(x_i) + \sum_{b+1}^{m} \bar{J}_k^{Pure}(x_i) \Big\}. \tag{20}$$

This gives the cost-to-go vector as

$$\hat{J}_k^*(x_i) = \begin{cases} \bar{J}_k^{Save}(x_i), & \text{if } x_i \in [x_1, x_{\hat{a}}] \\ \bar{J}_k^{Hybrid}(x_i), & \text{if } x_i \in [x_{\hat{a}+1}, x_{\hat{b}}] \\ \bar{J}_k^{Pure}(x_i), & \text{if } x_i \in [x_{\hat{b}+1}, x_m]. \end{cases} \tag{21}$$

The optimal driving mode at decision point k is thus given by

$$\hat{u}_k^*(x) = \begin{cases} Save, & \text{if } x \in [x_1, x_{\hat{a}}) \\ Hybrid, & \text{if } x \in [x_{\hat{a}}, x_{\hat{b}}) \\ Pure, & \text{if } x \in [x_{\hat{b}}, x_m]. \end{cases} \tag{22}$$

The latter step, i.e. Eq. (20), can be interpreted as minimizing the area below a curve defined by three separate segments; each corresponding to an interval in one of the three intermediate cost-to-go vectors, $\bar{J}_k^j$. This is illustrated in Figure 5, where the three intermediate cost-to-go vectors are depicted at a specific decision point. The conventional DP algorithm, given by Eq. (16), is in this case equivalent to minimizing the same area, but without any restriction on the number of segments, as is seen in Figure 4. However, despite the restrictions imposed on the cost-to-go, the suboptimal DP algorithm only increases the cost marginally, as seen in Fig. 6. This implies that overall fuel cost should not be affected very much by the suboptimal DP algorithm.

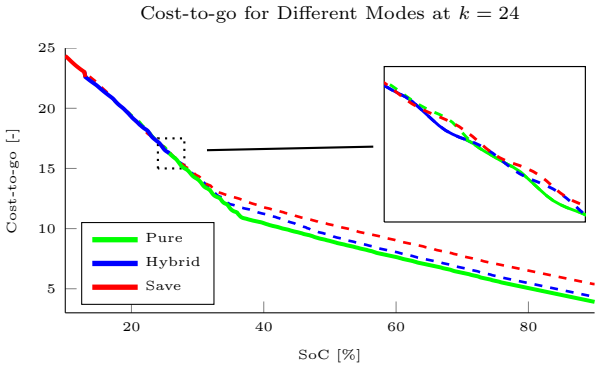

Fig. 5. Dotted lines represent the intermediate cost-to-go vectors, $\bar{J}_k^j$. The solid line illustrates the cost-to-go that minimises the area below the curve, $\hat{J}_k^*$.

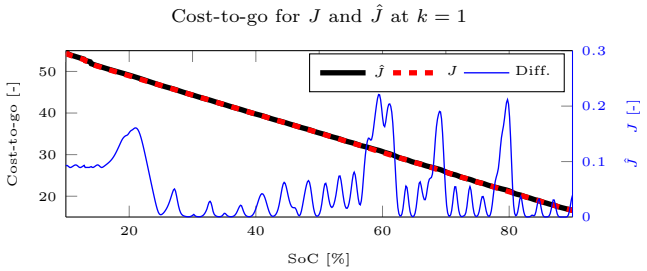

Fig. 6. Optimal and sub-optimal cost-to-go at $k = 1$.

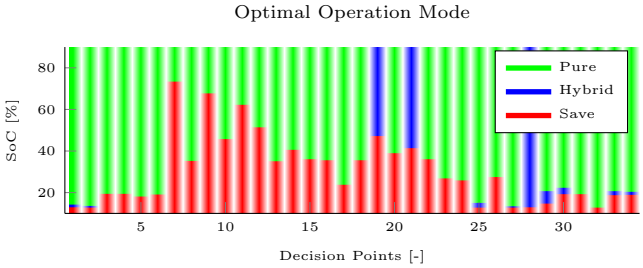

Fig. 7. Driving modes at the different decision points, as determined by the suboptimal DP algorithm.

6. SIMULATION STUDY

The commuter route shown in Figure 3 is considered in the simulation study and Figure 7 depicts the driving mode along the route, as determined by the suboptimal DP algorithm given by Eq. (18) - (22). The result is obtained by computing the optimal mode selection for all the 10 logged speed profiles shown in Figure 3; at each decision point k, the distribution of the optimal mode segments are determined by averaging over the results obtained for the individual speed profiles.

A different set consisting of 12 speed profiles, logged along the same commuter route, is then used for validation in the simulation study. The corresponding mode selection and the simulated SoC-trajectories are shown in Figures 8 - 9. In the figures it can be seen that the mode sometimes changes from *Pure* to *Hybrid* between two decision points; this occurs if the power demand of the drive cycle cannot be satisfied in *Pure*, i.e. the driving is more aggressive than anticipated. Nevertheless, the mode selection is quite

Table 3. Average fuel consumption and final SoC for the simulations with the mode selection algorithm, as shown in Fig. 9, and the CDCS strategy.

Strategy	Fuel [kg]	Final SoC [%]
CDCS	0.9760	20.57
Mode Selection	0.7741	20.22
	(-20.7 %)	

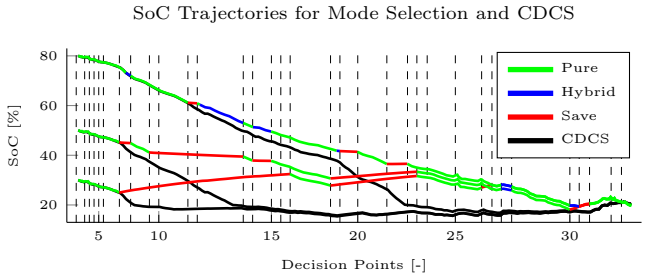

Fig. 8. SoC trajectories for the mode selection algorithm and the CDCS strategy for different inital SoC's.

predictable, in the sense that a similar sequence of modes is chosen along the route, provided that the starting SoC is similar. At 25 out of 34 decision points the same mode is selected for all simulations. *Pure* is by far the predominant mode, since the fuel cost is minimized if the battery is depleted at the end of the route. However, the *Save* mode is favoured during high power demands, clearly seen around decision point 20 (at 30-35 km), where there is uphill driving at high speeds. The *Hybrid* mode is almost never selected, implying that the heuristic used rule for engine on/off is not optimal in terms of fuel economy.

To illustrate the benefit with a route optimized mode selection, a comparison is made with the trivial Charge Depleting Charge Sustaining (CDCS) discharge strategy. The CDCS strategy is here implemented by the *Pure* mode followed by the *Hybrid* mode, when SoC drops below 0.2 for the first time. Table 3 summarizes the average fuel consumption and final SoC of the trips simulated along the route. Clearly an optimal selection of driving modes can decrease fuel consumption considerably, at least compared to the trivial mode selection used by the CDCS strategy. The absolute figures are, however, only of minor importance, as the heuristic rules within the driving modes are defined mainly for the sake of illustration.

7. CONCLUSION AND DISCUSSION

This paper has investigated the concept of optimal mode selection for a PHEV with driving modes that are defined by heuristic rules. A well known commuter route is considered and the driving mode is only allowed to change at a limited number of decision points along the route. The results indicate that an optimal mode selection can improve fuel economy substantially compared to a trivial mode selection strategy; the presented fuel savings are nevertheless of minor importance, as the heuristic rules in the paper are defined mainly to illustrate the concept. The main result in the paper is that if conventional DP is used to compute the optimal driving mode, it might lead to a counterintuitive mode selection. As a mode is not necessarily optimal over a connected set with respect

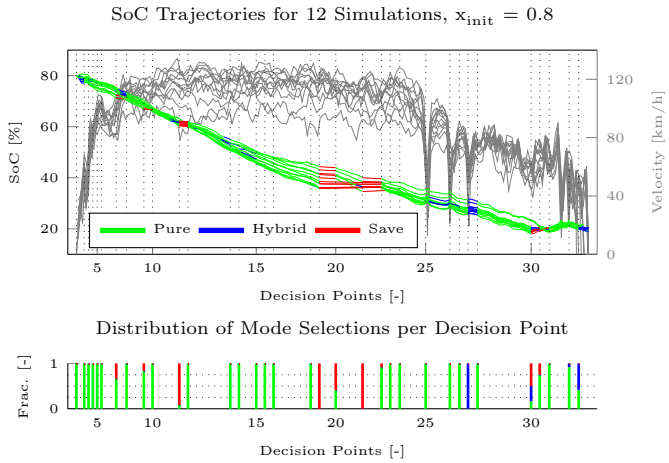

Fig. 9. SoC trajectories for 12 simulations along the route. The bar diagram illustrates the distribution of the mode selections at every decision point.

to battery SoC-level, at a specific decision point. To avoid such a solution a suboptimal DP algorithm is proposed, in which a driving mode is constrained to be "optimal" over a connected set with respect to battery SoC-level. The results indicate that the proposed algorithm is only slightly suboptimal compared to the conventional DP algorithm. Finally, it is worth to stress that optimal mode selection along a route with specified decision points is not very computationally demanding, even if DP is used. There is typically only a few driving modes to consider and a limited number of decision points.

REFERENCES

Bertsekas, D. (2000). *Dynamic Programming and Optimal Control*. Athena Scientific, Bellmont Massachusets.

Johannesson, L., Pettersson, S., and Egardt, B. (2009). Predictive energy management of a 4QT series-parallel hybrid electric bus. *Control Engineering Practice*, 17(12).

Karlsson, S. (2013). The Swedish car movement data project Final report. Technical Report, Chalmers University of Technology.

Opila, D.F., Aswani, D., McGee, R., Cook, J.a., and Grizzle, J. (2008). Incorporating drivability metrics into optimal energy management strategies for Hybrid Vehicles. *47th IEEE Conference on Decision and Control*.

Opila, D.F., Wang, X., McGee, R., Gillespie, R.B., Cook, J.a., and Grizzle, J.W. (2012). An Energy Management Controller to Optimally Trade Off Fuel Economy and Drivability for Hybrid Vehicles. *IEEE Transactions on Control Systems Technology*, 20(6).

Pisu, P., Koprubasi, K., and Rizzoni, G. (2005). Energy Management and Drivability Control Problems for Hybrid Electric Vehicles. *44th IEEE Conference on Decision and Control*.

Sciarretta, A. and Guzzella, L. (2007). Control of Hybrid Electric Vehicles. *IEEE Control Systems Magazine*, 27(2).

Wirasingha, S.G. and Emadi, A. (2011). Classification and Review of Control Strategies for Plug-In Hybrid Electric Vehicles. *IEEE Transactions on Vehicular Technology*, 60(1).